Heating and cooling of an office building using distributed heat pumps connected to a two-phase CO2 thermal management system: Detailed simulation

Sepehr Gholamrezaie[1], Massimo Cimmino[1], Parham Eslami-Nejad[1]
[1]Polytechnique Montréal, Montréal, Canada

Abstract

The increasing adoption of distributed heat pumps (DHPs) in buildings to improve energy efficiency presents an opportunity for effective thermal energy management. This study introduces an innovative approach that connects DHPs using a single pipe with two-phase CO2 as the heat transfer fluid, facilitating heat recovery between DHPs. The research involves a comprehensive semi-transient simulation of the entire system. The model comprises three key components: CO2 circulation system, an outdoor unit and the local units equipped with DHPs, all managed by specific control logics programmed to ensure optimal system operation. This model accounts for the complexities of heat distribution, heat transfer, CO2 circulation, and control mechanisms using newly developed Types in TRNSYS. The study presents a preliminary validation of the model's components against an experimental setup, alongside an examination of the model's capability to simulate a case study. This entails a presentation of the system's performance, demonstrating the potential of this innovative approach to examine thermal energy management in buildings.

Introduction

Thermal networks within buildings are crucial for advancing sustainable energy solutions, especially in heating and cooling applications. The main benefit of implementing a thermal network within a building lies in its ability to facilitate the transfer of thermal energy from one zone to another. For instance, heat absorbed from one zone to cool it down can effectively be transferred and utilized in another zone that requires heating. This strategy significantly increases energy efficiency by reducing the reliance on external energy sources. Thermal network systems can generally be categorized into two main groups: direct expansion systems and secondary loop systems.

Direct expansion systems include variable refrigerant flow (VRF) systems, which can provide simultaneous heating and cooling across various zones. VRF systems operate by adjusting the flow of refrigerant to indoor units based on the specific demand of each zone, offering precise temperature control but requiring intricate management of refrigerant flow. The advantage of VRF systems is the efficiency of the distribution of thermal energy in the building using latent heat. Secondary loop systems such as water loop heat pump systems, utilize a network of pipes to circulate a temperature source throughout the building. These systems facilitate the efficient transfer of thermal energy where needed, offering advantages in terms of easier control and operation. Distributed heat pumps (DHPs) within these networks connect to and utilize the secondary loop as a temperature source, simplifying the process of delivering consistent heating or cooling.

Given the ease of control associated with secondary loop systems, the advantage of utilizing the latent heat of a refrigerant and the environmental and operational benefits of using CO2, this study aims to explore the potential of CO2 thermal networks. Specifically, we investigate the configuration where DHPs are connected to a CO2 thermal network, aiming to analyse its impact on improving energy efficiency in building heating and cooling applications. This study represents a continuation of the research trajectory initiated by Eslami-Nejad et al. (2018). Their system, designed for comprehensive building thermal management, circulates two-phase CO2 through a single-pipe loop, integrating two local heat pumps and a water heater to address different thermal energy demands. Based on their initial concept, Eslami-Nejad and Bastani (2020) further explained the operational mechanics of the single-pipe CO2 thermal network. Their work highlighted its potential to enhance building energy performance through an energy balance approach, emphasizing the critical role of the CO2 circulation system's consistent performance alongside the building's simultaneous heating and cooling demands.

In a subsequent study, Bastani and Eslami-Nejad (2021) introduced a modeling technique aimed at simulating the system's application within office buildings across various Canadian climates. Employing a quasi-steady-state model, this analysis incorporated hourly thermal zone load profiles and weather data, uncovering significant energy performance optimization opportunities during shoulder seasons, particularly in milder climates like Vancouver's. This study was largely attributed to the favorable combination of warmer ambient temperatures and increased simultaneous heating and cooling demands. However, their study did not explore the dynamic behaviour of the system,

which involves considering zone capacities and integrating a model that includes thermostat control to more accurately resemble a realistic system.

Gholamrezaie et al. (2022) studied the simulation and control strategies applicable to a CO2 thermal network specifically for building thermal management in heating mode. Their approach utilized a semi-transient model implemented in TRNSYS with simplified component models. They showed that considering a minimum CO2 mass flow rate control strategy would help improve the system performance compared to a similar water loop system.

The current study endeavors to delve deeper into the complexity of the CO2 thermal management system. The focus is on detailing the system's concept, followed by a discussion on the modeling and validation of each component. By integrating more detailed component models, we aim to produce more realistic results, thereby refining our understanding of system behaviour across various operational scenarios. Moreover, this research seeks to broaden the applicability of the previous model, extending its functionality to provide the building load demands throughout all seasons.

Our thermal system is composed of three principal components as shown in Figure 1: CO2 circulation system located in mechanical room, the outdoor unit and the local units equipped with DHPs. The primary segment, located in the mechanical room, is tasked with delivering CO2 at a suitable mass flow rate and vapor quality, based on the building's thermal demand. The two-phase CO2 is circulated via a central loop, utilizing a single-pipe configuration. This design ensures efficient heat transfer by maintaining a constant source temperature for the DHPs located within the building. To achieve optimal comfort in each building zone, localized CO2-to-air HPs are directly connected to the loop. Within the loop connecting DHPs, two-phase CO2 undergoes condensation or evaporation at a steady temperature, closely matching typical indoor conditions (around 20°C). This facilitates year-round functionality without the necessity for thermal insulation, minimizing heat loss.

The CO2 circulation system is designed to replicate a reversible vapor compression cycle (RVCC). It includes a variable-speed compressor, an internal heat exchanger (IHE), a desuperheater (DSPHTR), electronic expansion valves (EEVs), pressure regulating valves (PRVs), and reversing valves (RVs). The desuperheater is crucial for reducing the temperature of the gas exiting the compressor and simultaneously preconditions incoming water or fresh air by leveraging the residual enthalpy of the CO2. Moreover, the outdoor unit functions as a gas cooler in conditions dominated by cooling and as an evaporator in those dominated by heating.

The operational framework of this system is segmented into three primary modes: heating (subdivided into heating-only and heating-dominant seasons), cooling (encompassing cooling-only and cooling-dominant periods), and a balanced mode where heating and cooling demands are equivalent. These modes are defined based on the net heat exchange within the CO2 thermal network via DHPs. Consequently, a net heat rejection into the CO2 thermal network signifies the system operates in cooling mode, while a net absorption signifies the system operates in heating mode.

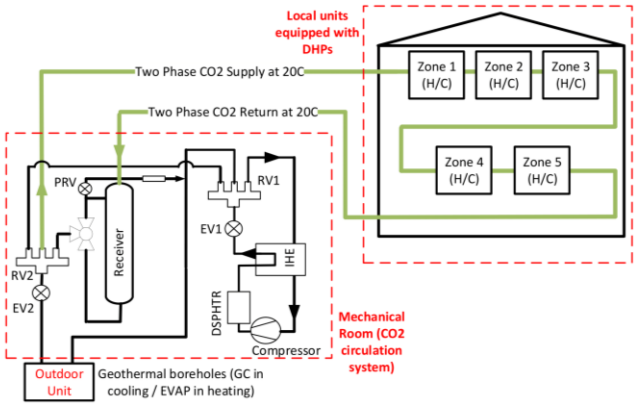

Figure 1 : Process flow diagram of the system

Model

A semi-transient methodology is employed to simulate the system's operation based on the hourly thermal load of each building zone. A modular approach is employed to model the entire thermal system, using a sub-model for each component of the system. These components are then interconnected through the input and output parameters within the TRNSYS simulation environment to simulate the entire system coupled to the building zones. Due to the limitations of the standard component libraries in TRNSYS in addressing the unique requirements of our system, custom models (referred to as "types" within TRNSYS) have been developed. The subsequent section delves into the detailed methodology employed to simulate each individual component.

Compressor model

The compressor model is developed based on a third-order polynomial, which is fitted to the manufacturer's data for a semi-hermetic reciprocating compressor capable of operating in transcritical mode for R744 refrigerant. This approach enables the representation of the compressor's performance across a range of operating conditions. The inputs to the model include suction pressure (P_{Suc}), discharge pressure (P_{dis}), and compressor speed in Hertz (Hz), which are critical parameters influencing the compressor's functionality.

The output from the model comprises two key parameters: the power input (W) performed by the compressor in kW and the CO2 mass flow rate ($\dot{m}$) in kg/hr. The equations governing the compressor model are as follows:

$$X = a_1 + a_2 * Hz + a_3 * Hz^2 + a_4 * Hz^3 + a_5 * P_{dis} + a_6 * P_{dis}^2 + a_7 * P_{dis}^3 + a_8 * P_{suc} + a_9 * P_{suc}^2 + a_{10} * P_{suc}^3 + a_{11} * Hz * P_{dis} + a_{12} * Hz * P_{dis}^2 + a_{13} * Hz * P_{suc} + a_{14} * Hz * P_{suc}^2 + a_{15} * Hz^2 * P_{dis} + a_{16} * Hz^2 * P_{dis}^2 + a_{17} * Hz^2 * P_{suc} + a_{18} * Hz^2 * P_{suc}^2 + a_{19} * P_{dis} * P_{suc} + a_{20} * P_{dis} * P_{suc}^2 + a_{21} * P_{dis}^2 * P_{suc} + a_{22} * P_{dis}^2 * P_{suc}^2 \quad (1)$$

where X can be the power input or the mass flow rate based on the constants defined in Table 1.

Table 1 : Compressor model coefficients

Coefficient	Value (Power input)	Value (Mass flow rate)
a_1	2.39E+01	3.43E+02
a_2	7.30E-02	7.36E+00
a_3	-8.74E-04	-7.70E-02
a_4	-1.99E-06	2.37E-04
a_5	-5.91E-03	-1.11E-01
a_6	2.93E-07	7.35E-06
a_7	6.68E-13	-6.93E-11
a_8	-1.03E-02	-1.84E-01
a_9	1.01E-06	2.79E-05
a_{10}	4.82E-13	-6.32E-10
a_{11}	3.05E-05	1.70E-04
a_{12}	-1.51E-09	-3.16E-08
a_{13}	-8.50E-05	-1.30E-03
a_{14}	9.62E-09	3.81E-07
a_{15}	-1.76E-07	-3.76E-06
a_{16}	1.28E-11	3.07E-10
a_{17}	9.25E-07	2.43E-05
a_{18}	-1.07E-10	-2.40E-09
a_{19}	2.73E-06	4.41E-05
a_{20}	-2.91E-10	-5.51E-09
a_{21}	-1.41E-10	-2.31E-09
a_{22}	1.57E-14	2.76E-13

Outdoor Unit

The outdoor unit consists of a plate heat exchanger assumed to be connected to a geothermal borehole. To simplify the model for the present study, it is assumed that the fluid (water/glycol) to the heat exchanger will be provided at constant temperature. Depending on the system's operational mode, the outdoor unit can function either as a gas cooler or as an evaporator. In the heating dominant mode, the system absorbs heat from outside. Conversely, in the cooling dominant mode, the system rejects heat to the outside and therefore operates as a gas cooler. Due to the operational differences between the gas cooler and evaporator, different models are proposed for each operational mode.

Gas cooler (GC)

The GC operates in a single-phase mode to cool down the CO2 (in vapor or supercritical state) to an appropriate temperature and at the same time preheat water for domestic use. Given that the outlet of the compressor may reside in the supercritical region, where the CO2 properties change rapidly, a discretized model has been implemented. In this discretization, the heat exchanger is divided into n nodes. At each node, the properties of the fluid are calculated, allowing for the determination of the heat transfer coefficient. Inputs to the model include CO2 pressure, enthalpy, mass flow rate, fluid (water/glycol) inlet temperature, and fluid (water/glycol) mass flow rate. For the gas cooler model the CO2 inlet conditions are determined by the DSPHTR CO2 outlet state. As outputs, the model provides CO2 enthalpy and pressure at the outlet of the heat exchanger, as well as the outlet fluid (water/glycol) temperature.

To model the heat exchanger, the energy equation is solved in an iterative backward scheme to satisfy the energy balance. The system of energy equations is as follows:

$$q(i) = \dot{m}_{CO2} \, (h_{i-1} - h_i)_{CO2} \quad (2)$$

$$q(i) = \dot{m}_{fluid} \, cp_{fluid} \, (T_i - T_{i+1})_{fluid} \quad (3)$$

$$q(i) = U_{tot}(i) * \frac{A}{n} \left(T_{CO2,i} - T_{fluid,i}\right) \quad (4)$$

Where *fluid* is the solution of 30% glycol/water mixture, U_{tot} is the heat transfer coefficient of the heat exchanger and A is the overall heat transfer area.

The selection of the appropriate heat transfer coefficient model is crucial for the accurate representation of the GC. Following a study by Kim and Park (2017) on single-phase convection heat transfer and pressure drop in brazed plate heat exchangers, the correlation proposed by Wanniarachcchi et al. (1995) for chevron-type plate heat exchangers is chosen for the GC. To calculate the CO2 heat transfer coefficient h_{CO2} at each node, the following equations are used:

$$m = 0.646 + 0.0011 * (90 - \beta) \quad (5)$$

$$Nu_t(i) = 12.6 * \phi^{(1-m)} * Re(i)^m * (90 - \beta)^{-1.14} \quad (6)$$

$$Nu_l(i) = 3.65 * \phi^{0.66} * Re(i)^{0.33} * (90 - \beta)^{-0.45} \quad (7)$$

$$Nu(i) = (Nu_t(i)^3 + Nu_l(i)^3)^{\frac{1}{3}} * \Pr(i)^{\frac{1}{3}} \quad (8)$$

$$h_{CO2}(i) = \frac{Nu(i) * k(i)}{Dh} \quad (9)$$

where Nu is the local Nusselt number, k is the thermal conductivity of CO2, Dh is the hydraulic diameter, β is the chevron angle of the plate heat exchanger ϕ is the enlargement factor, The Reynolds and Prandtl numbers are defined as follows:

$$\mathrm{Re}(i) = \frac{\dot{m}_{CO2} * Dh}{\mu(i) * b * W * NC} \quad (10)$$

$$\Pr(i) = \frac{cp_{CO2}(i) * \mu(i)}{k(i)} \quad (11)$$

where cp_{CO2} is the specific heat capacity of CO2, μ is the dynamic viscosity of CO2, b is the corrugation depth, W is the width of the plate heat exchanger and NC is the number of channels.

After calculating the heat transfer coefficient for each node, the overall heat transfer coefficient for each node $U_{tot}(i)$ is calculated based on the following equation:

$$U_{tot}(i) = \frac{1}{h_{CO2}(i)} + \frac{1}{h_{fluid}} + \frac{t}{k_{PHX}} \quad (12)$$

where h_{fluid} is the heat transfer coefficient of the fluid film and is considered constant and equal to 7000 W/m^2-K; t and k_{PHX} are the thickness and the thermal conductivity of the heat exchanger, respectively

Evaporator (EVAP)

The evaporator is modeled using the ε-NTU method thus the heat transfer rate is given by:

$$q = \varepsilon * C_{min} * \left(T_{\text{in,fluid}} - T_{\text{in,CO2}}\right)_{\text{evap}} \quad (13)$$

where $\varepsilon = 1 - e^{-NTU}$, $NTU = UA/C_{min}$ is the number of transfer units, U is the overall heat transfer coefficient calculated using Eq. (12), $C_{min} = \dot{m}_{fluid} * cp_{fluid}$, cp_{fluid} is the specific isobaric heat capacity of fluid, $T_{\text{in,fluid}}$, and $T_{\text{in,CO2}}$ are the inlet temperature of fluid, and CO2 to the evaporator respectively. It is assumed that the heat exchange process is adiabatic.

To calculate the heat transfer coefficient for the CO2 evaporation, the following correlation for overall Nusselt number ($\overline{Nu}$) is used (Lee et al., 2014):

$$\overline{Nu} = 98.7 \left(Re_{diff}^{-0.0848}\right)\left(Bo^{-0.0597}\right)\left(Xtt^{0.0973}\right) \quad (14)$$

$$Xtt = \left(\frac{1-x_m}{x_m}\right)^{0.87}\left(\frac{\rho_g}{\rho_f}\right)^{0.5}\left(\frac{\mu_f}{\mu_g}\right)^{0.12} \quad (15)$$

where x_m is the average CO2 quality, ρ is the density, $Re_{diff} = \frac{Re_g}{Re_f}$, $Bo = \frac{q''}{G * h_{fg}}$, $G = \frac{\dot{m}_{CO2}}{b*W*NC}$

Note that the subscripts g and f refer to saturated vapor and saturated liquid thermodynamic properties of the refrigerant, respectively.

Desuperheater (DSPHTR) model

Due to the similarity in the thermophysical properties of the gas cooler, we have utilized the same model for the desuperheater. However, the distinguishing factor lies in the boundary conditions applied to each model. For the desuperheater, the inlet conditions of the CO2 are known and are determined by the compressor's outlet conditions, including the CO2 mass flow rate, CO2 inlet pressure, and CO2 inlet enthalpy. On the fluid side, both the inlet temperature and the mass flow rate are specified. Additionally, the heat exchange process within the desuperheater is considered adiabatic.

Distributed Heat Pumps

The methodology for DHPs involves the modification of TRNSYS Type 919 to simulate a single-stage CO2-to-air heat pump. This heat pump conditions a moist air stream by either rejecting energy (in cooling mode) or absorbing energy (in heating mode) from two-phase CO2. The model relies on experimental data files containing the capacity (both total and sensible in cooling mode) and power normalized by their rated values. By inputting the mass flow rate, pressure, and enthalpy of the CO2, the model interpolates within the provided data to evaluate the capacity and power usage of the heat pump. This process enables the determination of the heat pump's energy consumption and the resulting thermodynamic state of the exiting CO2.

Building Zones

Building zones are represented through Type 690 in TRNSYS, a component designed to handle both sensible and latent loads through external inputs. It processes these loads by applying them to a simplified capacitance model of a building, effectively simulating the resulting temperatures and humidities. The model requires inputs of the loads along with an estimation of the building zone's thermal and moisture storage capacities, enabling it to compute the changes in zone temperature and humidity levels.

Control

The approach adopted in this study follows the procedure outlined by Gholamrezaie et al. (2022), wherein the control strategy is predicated upon the building's thermal demand. This involves using a controller to ensure that CO2 is supplied at the correct quality and mass flow rate. The goal is to keep the CO2 consistently within the saturation region of the loop, taking full advantage of the maximum enthalpy of evaporation/condensation at the loop's saturation temperature. Meanwhile, the DHPs will exchange heat with the loop at the lowest mass flow rate required to efficiently meet the thermal demands.

Experimental Validation

An experimental setup has been established at CanmetENERGY (Varennes). Preliminary experimental results are used here to validate the component models. In the experimental setup, the outdoor unit is emulated using a 10kW cooling/heating bath that can simulate varying environmental conditions. The setup also encompasses three simulated building zones to closely mimic real-life applications. Zone One is equipped with a water heater, providing a range of heating demands, while the remaining two zones feature CO2 to air heat pumps.

Test Procedure

For both the compressor and heat exchangers, our experimental procedure involves modulating the CO2 mass flow rate and pressure ratio and allowing the system to reach a steady state before data collection. Once stable operating conditions are achieved, data are recorded at 1-second intervals for a duration of 15 minutes. An average of the collected data set is then calculated for validation purposes. The primary data points gathered from the experimental setup include the power input of the compressor, the mass flow rates of CO2 and water measured by the flow meters, and the pressure and temperature measurements at the inlet and outlet of the components under test, utilizing pressure

meters and thermometers. The uncertainties associated with these measurements are listed in Table 2.

Table 2 : Measurement uncertainty

Instrument	Uncertainty
Temperature sensor	±0.10℃
Pressure meter	±0.08%
CO2 mass flow meter	±0.75%
Fluid mass flow meter	±0.10%
Wattmeter	±0.40%

Compressor

The compressor used in our experimental setup is a variable-speed reciprocating compressor. To validate our compressor model, we conducted tests across four distinct compressor speeds: 30 Hz, 36 Hz, 42 Hz, and 60 Hz. These speeds correspond to different mass flow rates, all maintained at the same pressure ratio, allowing for the investigation of the compressor's performance across a range of operating conditions. Each test setting was repeated across various pressure ratios. In total, the validation process was supported by 32 sets of experiments, providing a dataset for comparison.

Heat Exchangers

Our experimental setup employs plate heat exchangers for the heat transfer process. The specifications of these heat exchangers are detailed in Table 3. To validate our model of the heat exchangers, we focus on quantifying the energy exchanged with the water/glycol side. The heat exchanged (q_{fluid}) is calculated using the equation:

$$q_{fluid} = \dot{m}_{fluid}\, c_{p,fluid} \Delta T_{fluid} \quad (16)$$

where $\dot{m}_{fluid}$ represents the mass flow rate of the fluid, measured with a fluid flow meter, $c_{p,fluid}$ is the specific heat of the solution (30% glycol/water mixture), assumed constant at 3.9 kJ/kg-K, ΔT_{fluid} is the temperature difference between the inlet and outlet of the heat exchangers, measured using resistance temperature detectors (RTDs). Note that based on the uncertainty values introduced in Table 2, the uncertainty of equation 16, has a range of ±1.1% to ±9.2% according to the operation. Note that for validation of each heat exchanger 10 sets of experimental data is used.

Table 3 : Heat exchangers specifications

	DSPHTR	GC	EVAP
Length (mm)	314	314	314
Width (mm)	76	76	76
Number of plates	26	24	30
Plate thickness (mm)	0.3	0.3	0.3
Heat transfer area (m2)	0.47	0.42	0.54
Plate material	Copper	Copper	Copper

Results and Discussion

Model Validation

Compressor Model Validation

The validation of the compressor model focused on two key parameters: the power input to the compressor and the mass flow rate of CO2 circulated.

The comparison between the model predictions and experimental data for the compressor's power input is illustrated in Figure 2. This comparison demonstrated an agreement, with a maximum discrepancy of only 2.3%.

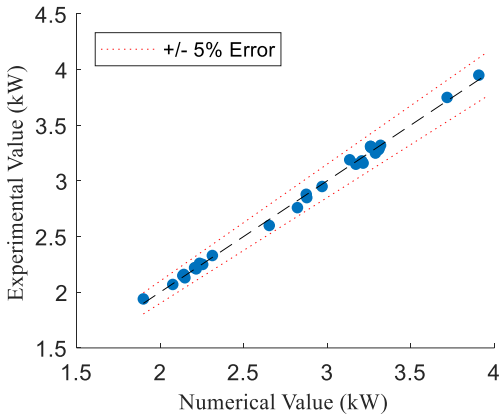

Figure 2 : Compressor model validation (power input correlation)

The validation of the mass flow rate produced by the compressor is depicted in Figure 3. Here, the model exhibits a good fit with the experimental data points, albeit with a maximum error of 15%. This increased variance, compared to that for the power input of the compressor, is partly due to the difficulty in maintaining steady conditions during tests. Variations in mass flow rates of approximately ±5% were observed during tests under similar operating conditions. Future work will focus on improving test conditions to minimize errors in measuring the mass flow rate.

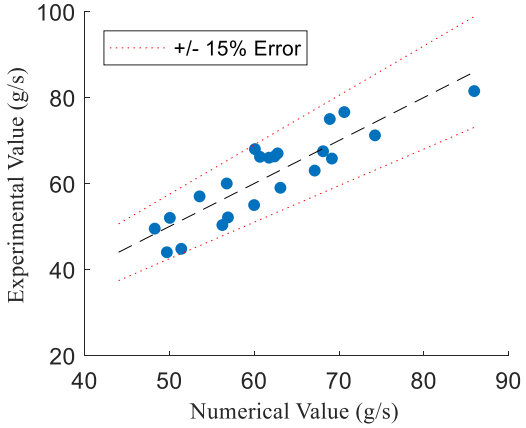

Figure 3 : Compressor model validation (mass flow rate)

Heat Exchangers Model Validation

To ensure the validation of the heat exchangers, the experimental setup was operated with specific conditions. The compressor speed was fixed at 30Hz for all tests. For evaluating the gas cooler (GC) and the desuperheater (DSHTR), the system was configured in cooling mode. This was achieved by closing the evaporator heat exchanger and opening the GC valve. Also, to add loads to the system one CO2 to air heat pump operated in cooling mode. Conversely, to assess the evaporator's performance, the system was set to a heating configuration by bypassing the GC and opening the evaporator valve, with considering CO2 to air heat pump operated in heating mode. During the validation process, 10 distinct sets of data were generated for each heat exchanger by adjusting the outlet temperature set point on the CO2 side. Across these tests, the output temperature of the heat exchangers was varied by changing the water flow rate to each heat exchanger. For the evaporator, the experimental procedure involved manually altering the setting of the expansion valve responsible and recording the resulting data. To validate the numerical model against experimental data, we calculated the heat transfer rate for each data set. Table 4 reports the maximum error, minimum error, and average error among the 10 sets of experiments compared to the model for each heat exchanger, highlighting the model's accuracy.

Table 4 : Heat exchangers validation

	Max_Error (%)	Min_Error (%)	AVE_Error (%)
DSPHTR	21.5	15	18.5
GC	26	16.1	20.2
EVAP	10.1	5.1	8

As the percentages indicate, the GC model exhibits the largest discrepancy among the modeled heat exchangers. This error can be attributed to the GC operating in the supercritical region and near the critical point of CO2. In this specified region, the thermodynamic properties of the refrigerant undergo rapid changes, which in turn results in a larger error margin.

A Case Study for Heating and Cooling Operations

To evaluate the model, the developed types in TRNSYS are utilized on a mid-sized office building located in Montreal, Canada. The layout of this office is divided into five specific sections, including a central core zone and four surrounding perimeter zones. Table 5 and Table 6 presents information about the floor dimensions and thermal capacities (TC) of each zone. Additionally, the same tables outline the characteristics of the loads, as detailed in the study by Tamasauskas, Kegel et al. (2018). Five DHPs are introduced, featuring specifications at a nominal source temperature of 19.8°C listed in Table 7.

Table 5 : Building specification (heating)

	West	South	East	North	Core
Total Demand [kWh]	2050	2198	1849	3020	1014
Peak Load [kW]	3.3	5.1	3.3	5.3	4.2
Total Demand Duration [h]	3692	2263	3352	2585	1267
Area [m^2]	67.2	113.4	67.2	113.5	150
TC [kJ/K]	2524	4256	2523	4256	5616

Table 6 : Building specification (cooling)

	West	South	East	North	Core
Total Demand [kWh]	2813	5122	2773	3732	6070
Peak Load [kW]	4.2	4.4	3.8	3.4	3.7
Total Demand Duration [h]	2482	4074	2816	3722	4885
Area [m^2]	67.2	113.4	67.2	113.5	150
TC [kJ/K]	2524	4256	2523	4256	5616

Table 7 : DHPs specification

	Heating Cap (kW)	Cooling Cap (kW)	COP_H	COP_C
Core	4.17	3.25	4.71	4.55
South	4.17	3.25	4.71	4.55
East	3.16	2.49	4.76	4.46
North	4.17	3.25	4.71	4.55
West	3.16	2.49	4.76	4.46

To illustrate the capabilities of the model, simulations are carried out for four distinct days throughout the year, each selected to represent the full spectrum of operational conditions the system might encounter: heating-only, cooling-only, heating-dominant, and cooling-dominant scenarios. For each of these scenarios, TRNSYS simulations are conducted using a time step of 7.5 minutes for the designated day. The system's performance is assessed using the coefficient of Performance (COP), which is defined as follows:

$$COP = \frac{\sum_{i=1}^{n}(|Q_{H,i}|+|Q_{C,i}|)+|Q_{Preheat}|}{E_{CO2\ Loop}+\sum_{i=1}^{n}E_{local\ HP,i}} \quad (17)$$

where $Q_{H,i}$ and $Q_{C,i}$ represent the total heat given to and absorbed from the zone *(i)* respectively, $E_{CO2\ Loop}$ is the absorbed power used by the main compressor to circulate CO2 in the loop, and $E_{local\ HP,i}$ is the power input to the local heat pump of the i^{th} zone.

Heating mode

Figure 4 depicts the model configuration for the heating mode, where all local heat pumps are operational in heating mode, with each process explained in Table 8. The control of the heating mode is dictated by the building's demand. Based on this demand, two parameters must be calculated: the CO2 mass flow and the quality of the CO2 inlet to the

loop (at point 5). These parameters are crucial for ensuring efficient operation and are controlled by the compressor speed and the high pressure respectively.

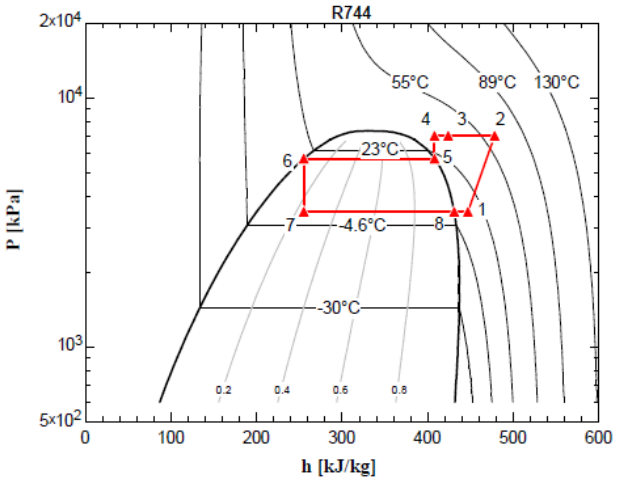

Figure 4 : Pressure-enthalpy diagram of the heating mode (at one time step)

It is important to note that the pressure ratio of the compressor depends on the size and inlet conditions of the DSPHTR, and the targeted DSHTR outlet temperature (for the discharge) and the EVAP size and inlet conditions (for the suction).

Table 8 : Heating mode thermodynamic process

Point	Component	Note
1-2	Compressor	$m_{CO2} = 350\ kg/hr$ $W = 3.01\ kW$
2-3	DSPHTR	$T_{fluid}(inlet) = 25℃$ $m_{fluid} = 100\ kg/hr$
3-4	IHE – high side	Supplies required heat needed for superheat
4-5	Expansion valve	Isenthalpic
5-6	CO2 loop	Constant temperature of 19.8℃
6-7	Expansion valve	Isenthalpic
7-8	EVAP	$T_{fluid}(inlet) = 15℃$ $m_{fluid} = 1500\ kg/hr$
8-1	IHE – low side	Absorb required heat needed for superheat of 10℃

The test has been recorded in heating mode for the coldest and a moderate day during the heating season. Table 9 demonstrates the system performance based on the number of heat pumps (HPs) running. The heating results indicate that the system's performance is dependent on the number of activated HPs. Furthermore, as we move towards balance with some HPs operating in cooling mode, the system utilizes more of the heat capacity of the thermal network, leading to an improvement in heat recovery.

Table 9 : Performance results for heating mode

Mode	COP
5 HPs on heating	3.6
4 HPs on heating – 1 HP cooling	4.3
3 HPs on heating – 2 HP cooling	5.1

Cooling mode

Figure 5 depicts the model configuration for the cooling mode, where all local heat pumps are operational in cooling mode, with each process explained in Table 10.

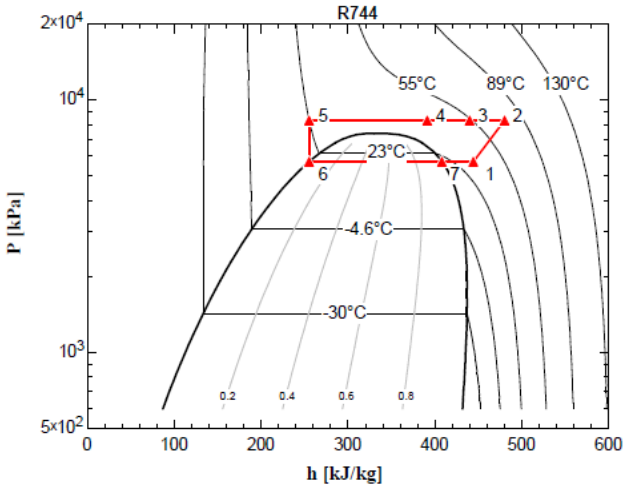

Figure 5 Pressure-enthalpy diagram of the cooling mode (at one time step)

In cooling mode, the high pressure is determined by the targeted outlet temperature (T_5) of the GC, as well as the conditions and parameters of the DSPHTR and GC. The concept is that the outlet temperature of the GC should reach the set point provided by the controller. Therefore, the pressure will adjust based on the water inlet condition and geometrical parameters of both the DSGTR and GC to achieve the targeted temperature (T_5). Furthermore, the low-pressure (compressor suction) will be the outlet of the CO2 network, which remains constant at 5.7 MPa.

Table 10 : Cooling mode thermodynamic process

Point	Component	Note
1-2	Compressor	$m_{CO2} = 310\ kg/hr$ $W = 2.3\ kW$
2-3	IHE – high side	Supplies required heat needed for superheat
3-4	DSPHTR	$T_{fluid}(inlet) = 25℃$ $m_{fluid} = 100\ kg/hr$

4-5	GC	$T_{fluid}(inlet) = 15℃$ $m_{fluid} = 1500\ kg/hr$
5-6	Expansion valve	Isenthalpic
6-7	CO2 loop	constant temperature of 19.8℃
7-1	IHE – low side	Absorb required heat needed for superheat of 10℃

The test was conducted in cooling mode for both the warmest and a moderate day during the cooling season. Table 11 demonstrates the system's performance in cooling mode across three different scenarios. The results are consistent with those observed in heating mode, indicating that moving towards a balanced mode results in a higher COP.

Table 11 Performance results for cooling mode

Mode	COP
5 HP on cooling	4.1
4 HP on cooling – 1 HP heating	4.9
3 HP on cooling – 2 HP heating	5.8

Conclusion

This study explores the innovative integration of distributed heat pumps within a single-pipe network using two-phase CO2 as the heat transfer medium, through both modeling and validation against an experimental setup. Initial validation of the system's components demonstrates that our model aligns closely with real-world systems, confirming its predictive capability. Furthermore, we examined the system's functionality in a simulated five-zone office building equipped with the proposed system, monitoring its performance and its capacity to seamlessly transition between operational modes. The preliminary results underscore the system's efficiency and adaptability, indicating promising potential for thermal management in buildings. Moving forward, we will focus on comprehensive validation of the entire system and a detailed investigation of the control parameters to enhance system performance and energy efficiency further.

Reference

Eslami-Nejad, P. ,Bastani, A, and Giguere, D (2018). Single pipe thermal energy system. N. Resources. Canada: WO2020/024050A024051.

Eslami-Nejad, P. and A. Bastani (2020). Two-phase CO2 loop for thermal energy management in buildings: Concept and building energy performance improvement. 14th Gustav Lorentzen Conference. Kyoto (Japan).

Bastani, A. and Eslami-Nejad, P (2021). CO2 Network for Thermal Management in Buildings. eSim Conference IBPSA-Canada. Vancouver (Canada).

Gholamrezaie, S, and Cimmino, M, and Eslami-Nejad, P (2022) Simulation and control strategy of a CO2 loop for building thermal management in heating mode. 15th IIR-Gustav Lorentzen Conference on Natural Refrigerants. Trondheim (Norway), 13-15 June 2022.

Tamasauskas, J., M. Kegel and J. Blake (2018). The Potential of Heat Pump Technologies for the Replacement of Rooftop Units in Small Commercial Buildings. eSim Conference IBPSA-Canada. Montreal (Canada), 9-10 May 2018.

Kim, M., and, Park, C., (2018). "An experimental study on single phase convection heat transfer and pressure drop in two brazed plate heat exchangers with different chevron shapes and hydraulic diameters" *Journal of Mechanical Science and Technology 31*, 2559-2571

Wanniarachchi, A S., and, Ratnam, U., (1995). "Approximate correlations for chevron-type plate heat exchangers", *30th National Heat Transfer Conference* New York (USA)

Lee, E., and, Kang, H., (2014). "Flow boiling heat transfer and pressure drop of water in a plate heat exchanger with corrugated channels at low mass flux conditions", *International Journal of Heat and Mass Transfer 77*, 37-45